DOI: 10.1002/asia.200700254

Synthesis of Oligo(thienylfuran)s with Thiophene Rings at Both Ends and Their Structural, Electronic, and Field-Effect Properties

Yasuo Miyata, Miki Terayama, Takeo Minari, Tohru Nishinaga, Takashi Nemoto, Seiji Isoda, and Koichi Komatsu*[a]

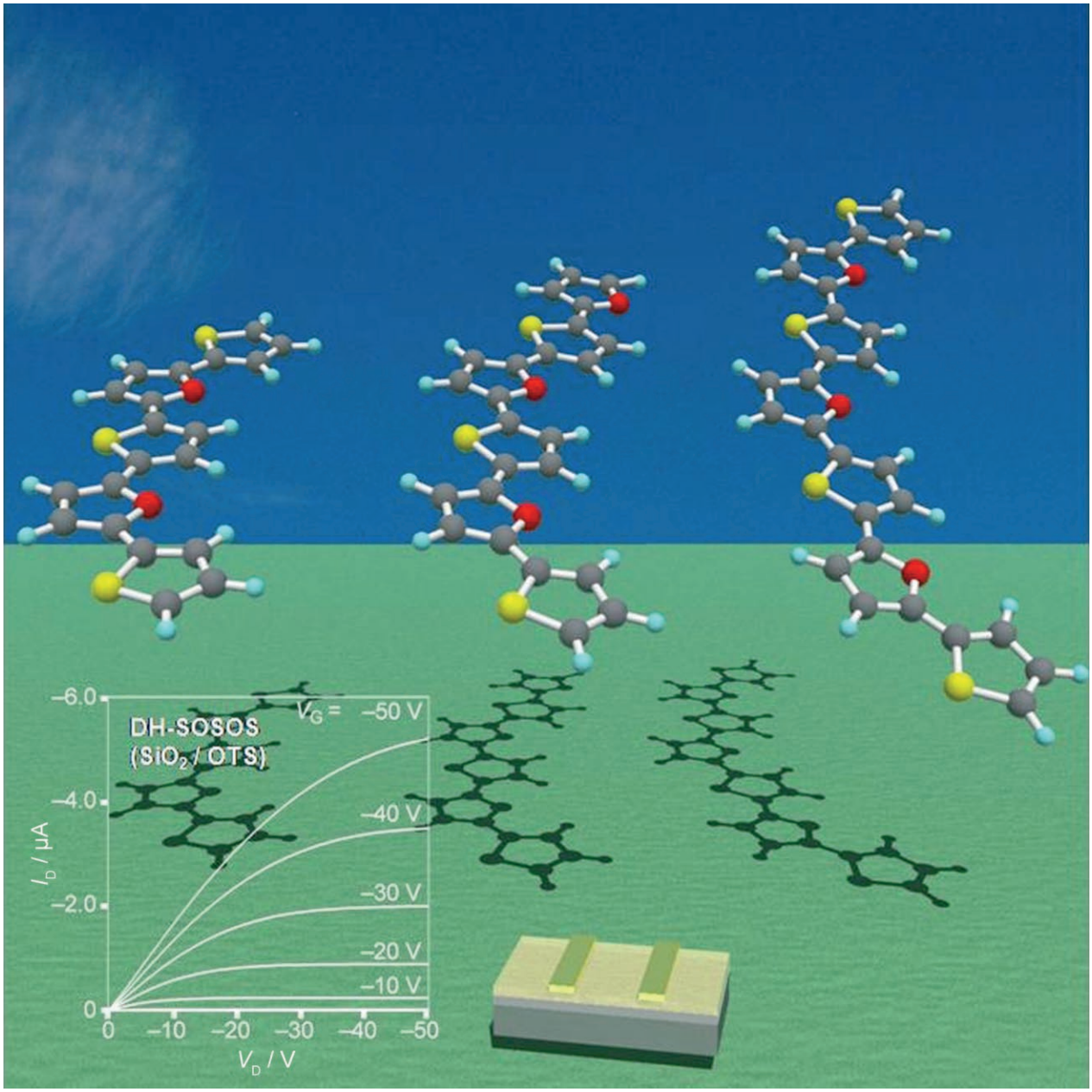

Abstract: Oligo(thienylfuran)s with thiophene rings at both ends (**SOSO-SOS**, **DE-SOSOS**, **DH-SOSOS**, **DE-SOSOSOS**, and **DH-SOSOSOS**; **S** and **O** denote thiophene and furan rings, respectively, **DE** and **DH** denote diethyl- and dihexyl-substituted, respectively) were newly synthesized by repetitive Stille coupling reactions. The UV/Vis maximum absorptions of the oligomers, **SO**, **SOSO**, **SOSOS**, **SOSOSO**, and **SOSOSOS**, exhibited a clear bathochromic shift with increasing number of heterocycles. The value of the oxidation peak potential (E_{pa}^{1}) determined by cyclic voltammetry decreased with an increase in the number of heterocycles by 0.06–0.08 V per heterocycle. The crystal-packing structures of **DE-SOSOS** and **DH-SOSOS** determined by X-ray crystallography have a herringbone motif and are denser than the reported structures of pentacene and α-sexithiophene. The morphologies of thin films prepared by vacuum deposition and spin coating were investigated by atomic force microscopy and X-ray diffraction. Among these films, those of **DE-SOSOS** and **DH-SOSOS** exhibited highly ordered arrangements. The devices based on vacuum-deposited and spin-coated films of **DE-SOSOS** and **DH-SOSOS** displayed the highest FET mobilities of 10^{-2}–10^{-3} $cm^2V^{-1}s^{-1}$ among the oligomers reported in this study.

Keywords: crystal packing · electronic properties · field-effect transistors · oligomerization · thin films

Introduction

Studies on organic field-effect transistors (OFETs) based on π-conjugated molecules such as oligoacenes[1] and parent oligothiophenes[2] have been actively carried out from the early 1990s and have been extensively conducted mostly in the form of vacuum-deposited thin films. Later, it was found that the films of α,α′-dialkylated oligothiophenes, produced not only by vacuum deposition[2a,c,d,f,h,3] but also by solution processes[2d,h,3b,4] such as spin coating and drop casting, can exhibit high mobility in OFETs. Thereafter, various π-conjugated compounds have been prepared, whose electronic and physical properties such as solubility and processability as well as their packing structures in the solid state were controlled by incorporation of heteroatoms and by substitution patterns. For example, high performance was demonstrated for OFETs made of vacuum- and solution-deposited thin films of compounds such as dinaphtho[2,3-*b*:2′,3′-*f*]thieno-[3,2-*b*]thiophene (**1**),[5] silylethynylated anthradithiophene (**2**),[6] 1,7-dicyanoperylene-3,4:9,10-bis(dicarboximide) **3**,[7] and so on.

Additionally, quinoidal terthiophenes with dicyanomethylene end groups[8] and oligothiophenes substituted with fluorinated alkyl[2h,9] and aryl[10] groups or with thermally removable groups to increase solubility[11] have been shown to be promising in FET performance. However, there has not been much study into the incorporation of other heteroaromatic rings such as furan into the oligothiophene π system, in spite of the possibility of the resulting system altering its electronic properties favorably to improve its FET properties.[12]

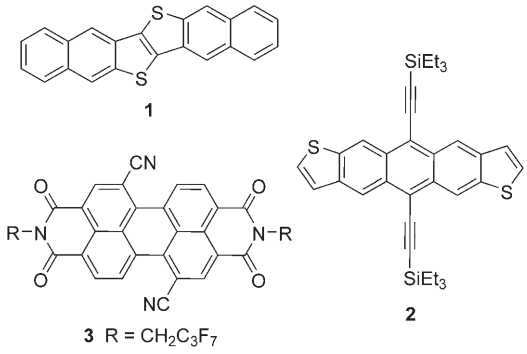

Previously, we synthesized three alternately connected thiophene–furan oligomers, that is, oligo(thienylfuran)s, with even numbers of heterocyclic rings (**SO**, **SOSO**, and **SOSOSO**; **S** and **O** denote thiophene and furan rings, respectively) and compared their structural and electronic properties with those of oligothiophenes with corresponding molecular size.[13] The properties of these oligomers were controlled by replacement of the sulfur atoms of every other thiophene unit by oxygen atoms. The energy levels of the highest occupied molecular orbitals (HOMOs) of the oligo-

[a] Dr. Y. Miyata, M. Terayama, Dr. T. Minari, Dr. T. Nishinaga, Dr. T. Nemoto, Prof. S. Isoda, Prof. K. Komatsu
Institute for Chemical Research
Kyoto University
Uji, Kyoto 611-0011 (Japan)
Fax: (+81) 774-38-3178
E-mail: komatsu@scl.kyoto-u.ac.jp

Supporting information for this article is available on the WWW under http://www.chemasianj.org or from the author.

(thienylfuran)s were found to be higher than those of the corresponding oligothiophenes, and the packing structure of **SOSO** determined by X-ray crystallography was denser than that of α-sexithiophene or pentacene. **SOSOSO** was also found to be readily soluble in common organic solvents such as CH_2Cl_2 and benzene, in sharp contrast to the intractably low solubility of α-sexithiophene. Thus, we expected that oligo(thienylfuran)s and their derivatives would be suitable as the active layer of OFET devices.

In the present study, we focused our attention on oligo(thienylfuran)s with thienyl rings at both ends (e.g., **SOSOS** and **SOSOSOS**), because such molecules are expected to be more robust than those with more-reactive furan rings at the ends. Furthermore, as it was reported that the field-effect properties of oligothiophenes are enhanced because of the improved capability for self-assembly when the terminal α and α′ positions are alkylated,[2a,d,f,h] ethyl- and hexyl-substituted oligo(thienylfuran)s (**DE-SOSOS**, **DE-SOSOSOS**, **DH-SOSOS**, and **DH-SOSOSOS**) were also prepared. The electronic properties of these oligo(thienylfuran)s were systematically investigated by means of cyclic voltammetry, UV/Vis spectroscopy, and theoretical calculations. Also, the X-ray crystallographic structures of **DH-SOSOS** and **DE-SOSOS** were determined and examined in detail. Finally, the FET characteristics and film morphologies of vacuum-deposited and/or spin-coated thin films were elucidated, which provide systematic information as to the FET characteristics of π-conjugated oligothiophene systems that contain furan structural units.

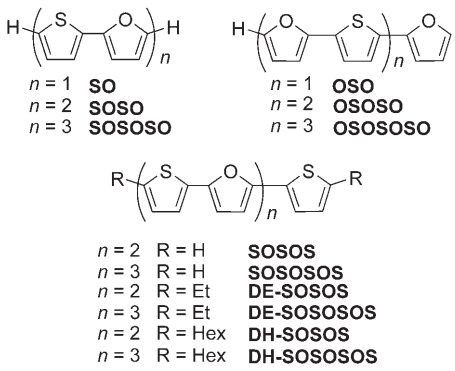

Results and Discussion

Synthesis

As shown in Scheme 1, α,α′-dialkylated and parent oligo(thienylfuran)s consisting of five and seven heterocycles were synthesized from α-alkylated thiophenes **1a** and **1b** and thienylfuran **4c**[13] as starting materials by the Stille cross-coupling technique. It is known that the two C–H bonds at the α and α′ positions in the π-conjugated oligo-

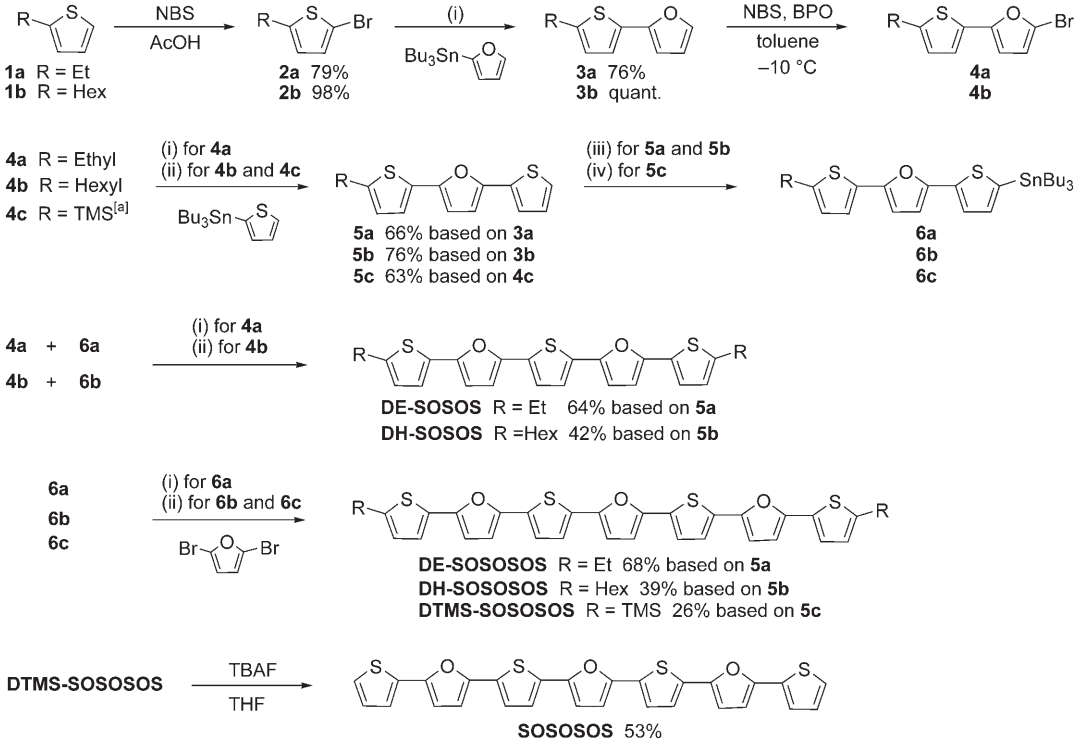

Scheme 1. Synthesis of α,α′-dialkylated oligo(thienylfuran)s with five and seven heterocycles. Reaction conditions: (i) $[Pd(PPh_3)_4]$, CuO, DMF, 100 °C, 1 h.[15] (ii) $[Pd(PPh_3)_4]$, THF, 70 °C, 2–3 days. (iii) 1) LDA, THF, −78 °C; 2) Bu_3SnCl, −78 °C→room temperature. (iv) 1) *n*BuLi, TMEDA, THF, −78 °C; 2) Bu_3SnCl, −78 °C→room temperature. BPO = benzoyl peroxide, DMF = *N*,*N*-dimethylformamide, LDA = lithium diisopropylamide, NBS = *N*-bromosuccinimide, TBAF = tetra-*n*-butylammonium fluoride, TMEDA = *N*,*N*,*N*′,*N*′-tetramethylethylenediamine, TMS = trimethylsilyl. [a] See reference [13].

CHEMISTRY
AN ASIAN JOURNAL

mers of five-membered heterocycles tend to be dibrominated (and dilithiated), even when 1 equivalent of reagent is employed, as the chain length becomes longer.[12c,14] Therefore, one side of **5c** was protected by a TMS group to secure monolithiation for the following stannylation to give **6c**.

All oligo(thienylfuran)s were constructed by using bromides **4a–c** and stannyl compounds **6a–c** as building blocks. Bromides **4a** and **4b** were quite unstable and had to be used immediately without purification in the next cross-coupling reaction. The α,α′-dialkylated oligomers composed of five heterocycles (**DE-SOSOS** and **DH-SOSOS**) were obtained by palladium-catalyzed Stille cross-coupling of **4a** and **4b** with **6a** and **6b**, respectively. Stannyl compounds **6a–c** were also subjected to Stille coupling with 2,5-dibromofuran to give oligomers composed of seven heterocycles (**DE-SOSOSOS**, **DH-SOSOSOS**, and **DTMS-SOSOSOS**). The unsubstituted oligomer **SOSOS** was synthesized according to a literature procedure.[12b] Two types of Stille coupling conditions were employed: α,α′-diethyl-substituted oligomers were prepared in the presence of CuO (Scheme 1, condition (i)),[15] and α,α′-dihexyl derivatives and **DTMS-SOSOSOS** were prepared in the absence of CuO (Scheme 1, condition (ii)). Whereas the cross-coupling in the absence of CuO required 2–3 days for consumption of all the starting material, only 1 h was sufficient for the reaction in the presence of CuO. The product yields were higher with condition (i) (61–68%) than with condition (ii) (26–63%). The unsubstituted oligomer **SOSOSOS** was obtained by desilylation of **DTMS-SOSOSOS**.

In contrast to the intractably low solubility of the parent α-sexithiophene ($<0.05\ mg\,mL^{-1}$ in CH_2Cl_2),[16] **SOSOSOS** is readily soluble in CH_2Cl_2 with a concentration of approximately $10\ mg\,mL^{-1}$ or slightly higher. Also, the melting point of **SOSOSOS** (179.4–181.3 °C) is significantly lower than that of the parent α-septithiophene (328 °C).[17] The melting points of **DE-SOSOSOS** (172.9–174.3 °C) and **DH-SOSOSOS** (137.3–139.1 °C) are even lower than that of **SOSOSOS**. The same trend was observed in the case of the oligomers containing five heterocycles (see Experimental Section).

Absorption Spectra

The observed UV/Vis longest-wavelength absorptions (λ_{max}) of oligo(thienylfuran)s with thiophene at both ends are summarized in Table 1 together with the data for oligo(thienylfuran)s (**SO**, **SOSO**, and **SOSOSO**)[13] and those with furan at both ends (**OSO**, **OSOSO**, and **OSOSOSO**)[12c] for comparison. As shown clearly in Figure 1, λ_{max} exhibits a bathochromic shift with an increase in the number of heterocycles. There is almost no difference in maximum absorption between oligo(thienylfuran)s with furan rings at both ends (**OSO**, **OSOSO**, and **OSOSOSO**) and those with thiophene rings at both ends as long as the total number of heterocycles is the same. The Kohn–Sham (KS) HOMO and LUMO (lowest unoccupied molecular orbital) levels and the HOMO–LUMO gaps of these oligomers were estimated by

Table 1. Observed longest-wavelength absorptions (λ_{max}) and calculated Kohn–Sham HOMOs, LUMOs, and HOMO–LUMO gaps of the oligomers composed of alternately connected thiophene and furan rings.

Compound	λ_{max} [nm]	HOMO[a] [eV]	LUMO[a] [eV]	HOMO–LUMO gap[a] [eV]
SO	298[b]	−5.69	−1.43	4.26
SOS	366[c]	−5.33	−1.82	3.51
OSO	362[c]	−5.33	−1.82	3.51
SOSO	387[b]	−5.14	−2.04	3.10
SOSOS	415[d]	−5.03	−2.17	2.86
OSOSO	413[c]	−5.03	−2.17	2.86
SOSOSO	432[b]	−4.96	−2.26	2.70
SOSOSOS	447[d]	−4.91	−2.33	2.58
OSOSOSO	447[b]	−4.91	−2.32	2.57
DE-SOSOS	420[d]			
DH-SOSOS	421[d]			
DE-SOSOSOS	451[d]			
DH-SOSOSOS	451[d]			

[a] Calculated at the B3LYP/6-311+G(2d,p)//B3LYP/6-31G(d) level. [b] Measured in THF.[13] [c] Measured in CH_2Cl_2.[12] [d] Measured in THF.

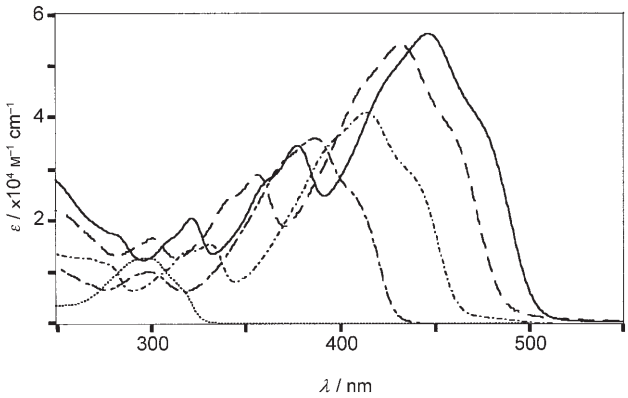

Figure 1. UV/Vis absorption spectra of **SO** (•••••), **SOSO** (– – –), **SOSOS** (–•–•–), **SOSOSO** (– – –), and **SOSOSOS** (——) measured in THF.

calculations at the B3LYP/6-311+G(2d,p)//B3LYP/6-31G(d) level and are also shown in Table 1. These results are in good agreement with the observed trend: as the number of heterocycles increases, the HOMO–LUMO gap becomes smaller, irrespective of the type of heterocycle involved. The maximum absorptions of α,α′-alkylated oligomers were bathochromically shifted by 4–6 nm compared with those of the corresponding parent oligomers, in the same way as previously reported for oligothiophenes.[18]

Electrochemistry

Cyclic voltammetry (CV) of oligo(thienylfuran)s with thiophene at both ends was carried out in CH_2Cl_2. The oxidation potentials (E_{pa} and $E_{1/2}$) are listed in Table 2 together with those of **SOSO** and **SOSOSO** for comparison.[13] In contrast to the voltammograms of oligomers with a furan ring at the end (**SOSO** and **SOSOSO**), which exhibited only one irreversible peak, the voltammogram of that with thiophene rings at both ends (**SOSOS**)[19] as well as those with alkyl groups at the α and α′ positions (**DE-SOSOS** and **DH-SOSOS**) exhibited two reversible oxidation waves, which

Table 2. Oxidation potentials[a] (E_{pa} and $E_{1/2}$) of the oligomers composed of alternately connected thiophene and furan rings.

Compound	E_{ox}^1		E_{ox}^2	
	E_{pa} [V]	$E_{1/2}$ [V]	E_{pa} [V]	$E_{1/2}$ [V]
SOSO	+0.42[b]	–[c]	–[d]	–[d]
SOSOS	+0.36	+0.29	+0.68	+0.57
DE-SOSOS	+0.27	+0.20	+0.59	+0.52
DH-SOSOS	+0.24	+0.20	+0.57	+0.51
SOSOSO	+0.29[b]	–[c]	–[d]	–[d]
SOSOSOS	+0.21	–[c]	+0.56	–[c]
DE-SOSOSOS	+0.12	–[c]	+0.35	–[c]
DH-SOSOSOS	+0.14	+0.09	+0.39	–[c]

[a] Measured in CH_2Cl_2 versus Fc/Fc^+ (Fc = ferrocenyl). [b] Reference [13]. [c] No reversible wave was observed. [d] Not observed.

correspond to the successive formation of a stable radical cation and a dication. On the other hand, whereas the voltammograms of **SOSOSOS** and **DE-SOSOSOS** showed two irreversible oxidation peaks, that of **DH-SOSOSOS** exhibited one reversible wave and one irreversible peak. Apparently, hexyl groups are more advantageous than ethyl groups in preventing the decomposition of the radical cation, which probably occurs by polymerization. The dication of **DH-SOSOSOS** appears to be less stable than those of **DE-SOSOS** and **DH-SOSOS**, although an adequate rationale for this observation cannot be found at present.

Among the parent oligo(thienylfuran)s, the value of the first oxidation peak potential, E_{pa}^1, was lowered by 0.06–0.08 V for each increase of one heterocycle. This trend is in agreement with the energy levels of the HOMOs estimated by DFT calculations shown in Table 1. The donor ability of two alkyl groups at the α and α′ positions also lowered E_{pa}^1 by 0.07–0.12 V for both **SOSOS** and **SOSOSOS**.

Crystal Structures of DH-SOSOS and DE-SOSOS

As reported previously, single crystals of **SOSO** were successfully obtained by sublimation under a low pressure of nitrogen (400 Pa), and its X-ray structure was determined.[13] Similarly, single crystals of oligomers composed of five heterocycles with hexyl and ethyl groups at the α and α′ positions, **DH-SOSOS** and **DE-SOSOS**, were obtained by sublimation at 200 and 150 °C, respectively, under reduced pressure (133 Pa) for 10 days. The molecular structures were determined by X-ray crystallography at −173 °C.

The ORTEP drawing of the heterocyclic pentamer with hexyl groups at the α and α′ positions, **DH-SOSOS**, exhibited an all-*transoid* conformation and a nearly planar structure, although the molecules are slightly bent (Figure 2). The dihedral angles between the mean planes of the heterocycles are A–B 5.09(54), B–C 5.10(48), C–D 2.41(44), and D–E 11.99(42)°. The crystal-packing structure is of a herringbone arrangement similar to the cases of oligothiophenes[18b,20] and pentacene[20f] (Figure 3). No specific intermolecular contact between chalcogen atoms was observed, but the shortest intermolecular contact between the π-conjugated cores was shown to be 3.31 Å between C3 (C3′) of one molecule and C6 (C6′) of an adjacent molecule

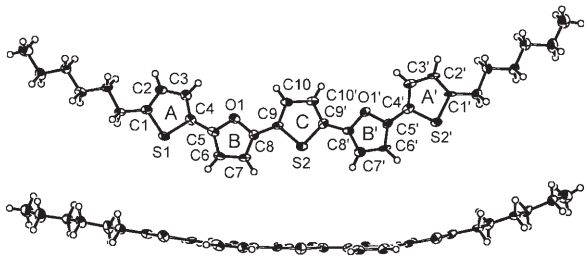

Figure 2. ORTEP drawing of **DH-SOSOS** (top and side views). Thermal ellipsoids are drawn at the 50% probability level.

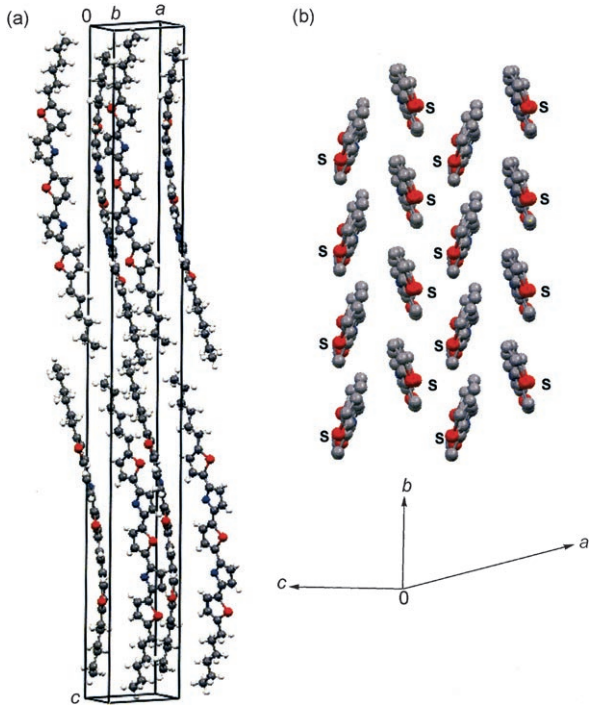

Figure 3. Packing structures of **DH-SOSOS** viewed with a) the *c* axis vertical and b) the *b* axis vertical. Hexyl substituents and hydrogen atoms are omitted for clarity. The unit-cell parameters (monoclinic $P2_1/n$) are $a = 7.416(3)$, $b = 5.879(2)$, $c = 64.92(2)$ Å, $\beta = 91.815(6)°$, and $Z = 4$.

(Figure 4, distance **A**) and 3.39 Å between C7 (C7′) of one molecule and C8 (C8′) of an adjacent molecule (Figure 4, distance **B**). Both values are shorter than the sum of the van der Waals (vdW) radii of sp^2-hybridized carbon atoms (3.40 Å)[21] and are even smaller than the shortest intermolecular contact between the carbon atoms of the π-conjugated cores (3.50 Å) in α,α′-dimethylquaterthiophene,[20a] whose alkyl groups are less bulky than those in **DH-SOSOS**.

On the other hand, the crystal structure of the same pentamer with ethyl substituents, **DE-SOSOS**, involved statistical disorder at the terminal thiophene rings, which arise from the 180° rotation around the C16–C17 (C16–C17′) bond connecting the D and E rings (Figure 5a and b), and the *transoid* (*t*) conformer (Figure 5a) was found to dominate over the *cisoid* (*c*) (Figure 5b) on the basis of diffrac-

CHEMISTRY
AN ASIAN JOURNAL

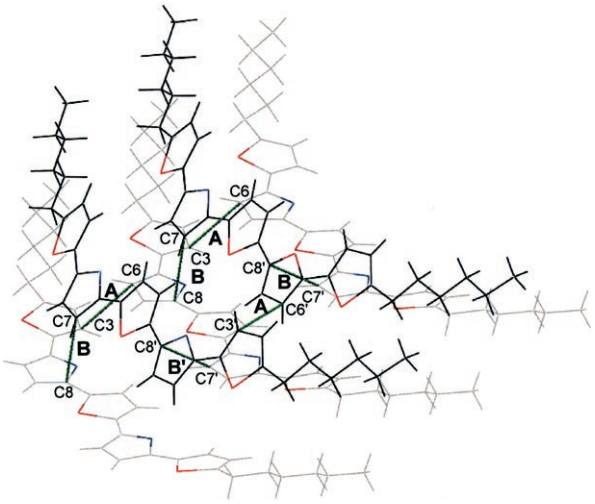

Figure 4. Packing structure of **DH-SOSOS**. Sulfur and oxygen atoms are shown in red and blue, respectively. The green lines **A** and **B** indicate the shortest intermolecular contacts between π-conjugated cores: 3.31 Å between C3 and C6 (C3′ and C6′) of adjacent molecules and 3.39 Å between C7 and C8 (C7′ and C8′) of adjacent molecules, respectively.

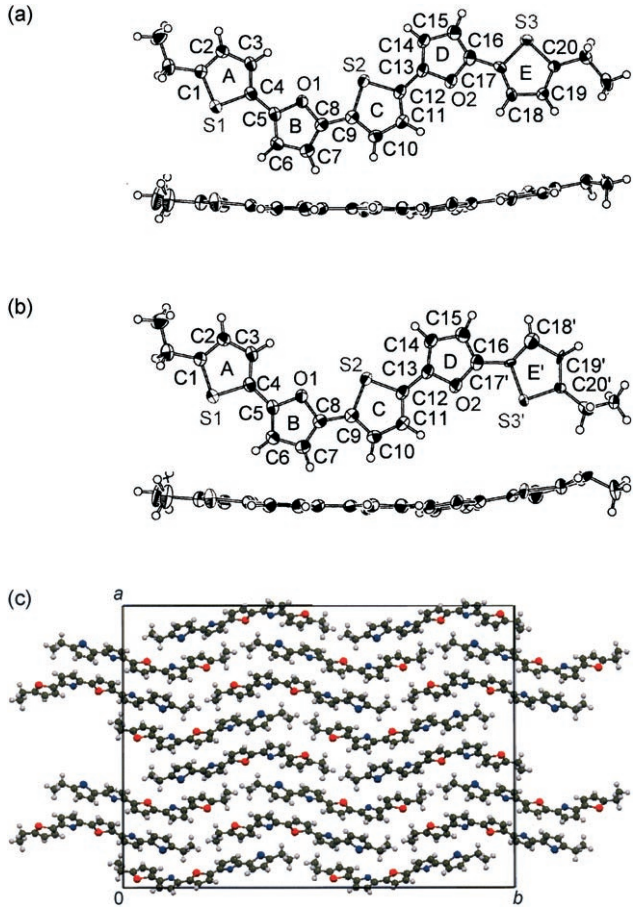

Figure 5. ORTEP drawings (top and side views) of a) the *transoid* (*t*) conformer and b) the *cisoid* (*c*) conformer of **DE-SOSOS**. Thermal ellipsoids are drawn at the 50% probability level. c) Packing structure within the *ab* plane of the *t* conformer of **DE-SOSOS**. The unit-cell parameters (orthorhombic *Fdd*2) are $a=32.160(8)$, $b=45.189(11)$, $c=5.7411(15)$ Å, and $Z=16$.

tion data ($t/c=3:1$). Apart from this disorder, the conformation between the B and C rings was found to be *cisoid*, whereas that between A and B as well as C and D was *transoid*. This is in contrast to the structure of **DH-SOSOS** and **SOSO**, in which all the heterocycles are connected in a *transoid* fashion.[13] Although the molecules are very slightly bent (Figure 5), their planarity is fairly good as shown by the generally minute dihedral angles between the mean planes: A–B 5.42(13), B–C 3.76(13), C–D 8.02(13), D–E 8.43(37), and D–E′ 3.21(86)°. Among these, the twist angle (dihedral angle) for the bonds connecting the rings in the *cisoid* conformation appears to be slightly smaller.[22] The distances between O1 and S2 in the B and C rings and O2 and S3′ in the D and E′ rings were shown to be 2.98 and 3.10 Å, respectively, both of which are shorter than the sum of the vdW radii of oxygen and sulfur atoms (3.32 Å).[21] This suggests the possibility of intramolecular contact between these heteroatoms. Notably, single crystals can also be obtained by slow evaporation of **DE-SOSOS** in CH_2Cl_2/diethyl ether (1:1), and X-ray crystallography of these crystals revealed exactly the same molecular conformation, disorder, and packing as the crystals obtained by sublimation. This fact in particular implies that the crystal-packing force is the dominant factor for the geometrical arrangement in the present system, which is to be compared with the all-*transoid* conformation observed for the crystal structures of **DH-SOSOS**, **SOSO**,[13] and α-oligothiophenes.[18b,20] As shown in Figure 5c, the crystal-packing structure of **DE-SOSOS** is of a herringbone arrangement similar to that of **DH-SOSOS**, **SOSO**,[13] and α-oligothiophenes.[18b,20] Whereas the crystal structures of these latter oligomers contain monoclinic unit cells, that of **DE-SOSOS** contains an orthorhombic unit cell consisting of 16 molecules. As with the case of **DH-SOSOS**, no intermolecular interaction between chalcogen atoms was observed, and intermolecular contacts between π-conjugated cores shorter than the sum of the vdW radii were found to be 3.23 Å between C3 of one molecule and C6 of an adjacent molecule (Figure 6, distance **A**) and 3.34 Å between C10 of one molecule and C16 of an adjacent molecule (Figure 6, distance **B**).

To illustrate the herringbone packing of these oligomers, the crystal structure of the **SOSOS** skeleton of dihexyl derivative **DH-SOSOS** is shown in Figure 7, together with the observed values of the herringbone angle and the intermolecular distances. These values are smaller than the corresponding values for pentacene[20f] and α-sexithiophene,[20f] and larger than those of **SOSO** apart from distance (ii),[13] thus indicating that the packing structure of **DH-SOSOS** is tighter than that of pentacene and α-sexithiophene and looser than that of **SOSO** (Table 3). The packing structure of diethyl derivative **DE-SOSOS** showed a trend similar to that of **DH-SOSOS**. These observations indicate that the replacement of some of the sulfur atoms of oligothiophene by oxygen atoms causes denser crystal packing, as was shown in the packing structure of **SOSO**.[13]

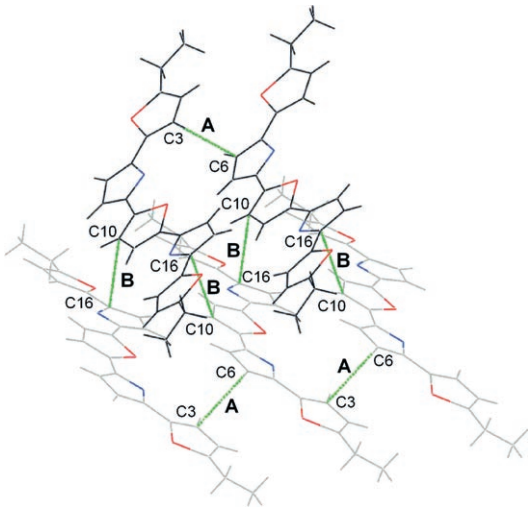

Figure 6. Packing structure of the *t* conformer of **DE-SOSOS**. Sulfur and oxygen atoms are shown in red and blue, respectively. The green lines **A** and **B** indicate the shortest intermolecular contacts between π-conjugated cores: 3.23 Å between C3 and C6 of adjacent molecules and 3.34 Å between C10 and C16 of adjacent molecules, respectively.

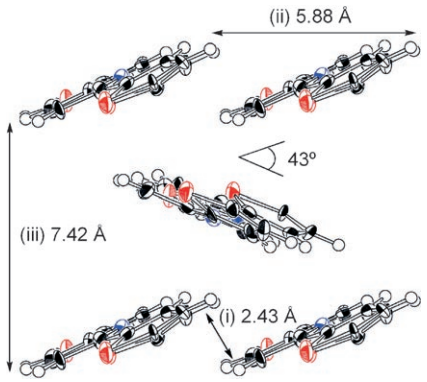

Figure 7. Herringbone angle and intermolecular distances of **DH-SOSOS**. Hexyl substituents are omitted for clarity.

Table 3. Herringbone angles and intermolecular distances (i)–(iii) in Figure 7 determined from the crystal packings of **DH-SOSOS**, **DE-SOSOS**, **SOSO**, α-sexithiophene, and pentacene.

Compound	Herringbone angle [°]	Intermolecular distance (i) [Å]	(ii) [Å]	(iii) [Å]
DH-SOSOS	43	2.43	5.88	7.42
DE-SOSOS	62	2.39	5.74	7.83
SOSO[a]	50	2.66	5.68	7.28
α-Sexithiophene[b]	65	3	6.0	7.9
Pentacene[b]	53	2.63	6.27	7.78

[a] Reference [13]. [b] Reference [20].

Film Morphology

To characterize further the molecular structures of these oligomers in the bulk, we investigated the morphologies of thin films vacuum-deposited and spin-coated on Si/SiO_2 substrates by atomic force microscopy (AFM) and X-ray diffraction (XRD). The observed film morphologies are summarized in Table 4.

Among the thin films of the parent oligomers formed by vacuum deposition, the film morphology of the shortest-chain oligomer **SOSOS** was poor, and only microcrystals on an amorphous layer were observed in the AFM image (Figure 8a). In contrast, AFM images of the films of the longer-chain oligomers **SOSOSO** and **SOSOSOS** as well as the alkylated derivatives **DE-SOSOS** and **DH-SOSOS** showed layer-by-layer arrangements that consist of grains 1–2 μm^2 in size (Figure 8b–e). Although the XRD pattern of the thin film of **SOSOSOS** did not exhibit a clear peak, AFM images of **DE-SOSOS** and **DH-SOSOS** showed the formation of highly ordered thin films (Figure 8d and e). As shown in Figure 9a, the XRD pattern of a thin film of **DE-SOSOS** showed a diffraction peak at $2\theta = 3.74°$ (100), corresponding to a *d* spacing of 23.5 Å. This is only 0.9 Å larger than half the unit-cell length along the *b* axis (22.6 Å),[23] along which the two molecules are aligned in series (Figure 5c) in the crystal packing (see above). Therefore, the observed *d* spacing is considered as related to the length of one molecule. Similarly, the diffraction peak in the XRD profile of the film of **DH-SOSOS** (Figure 9b) was observed at $2\theta = 2.88°$ (100), corresponding to a *d* spacing of 30.6 Å. As the molecular length of all-*trans* **DH-SOSOS** was estimated to be

Table 4. Film morphologies of oligomers observed by scanning AFM.

Compound	Film morphology	
	Vacuum deposition	Spin coating
SOSOS	amorphous	amorphous
SOSOSO	layer-by-layer	–[a]
SOSOSOS	layer-by-layer	layer-by-layer
DE-SOSOS	layer-by-layer	–[a]
DH-SOSOS	layer-by-layer	layer-by-layer
DE-SOSOSOS	amorphous	–[a]
DH-SOSOSOS	amorphous	amorphous

[a] No observation made.

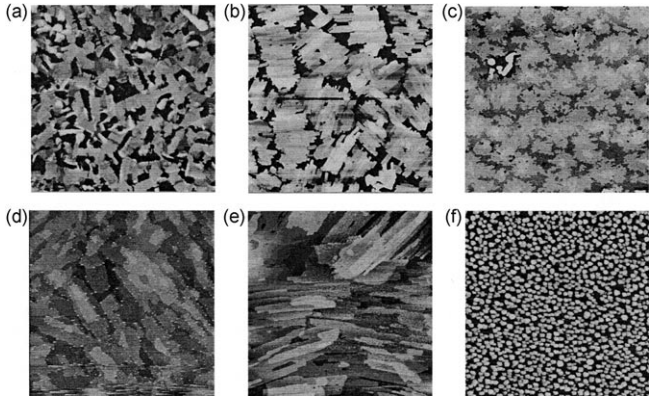

Figure 8. AFM images ($10 \times 10\ \mu m^2$) of thin films formed by vacuum deposition. a) **SOSOS**, b) **SOSOSO**, c) **SOSOSOS**, d) **DE-SOSOS**, e) **DH-SOSOS**, and f) **DH-SOSOSOS**.

CHEMISTRY
AN ASIAN JOURNAL

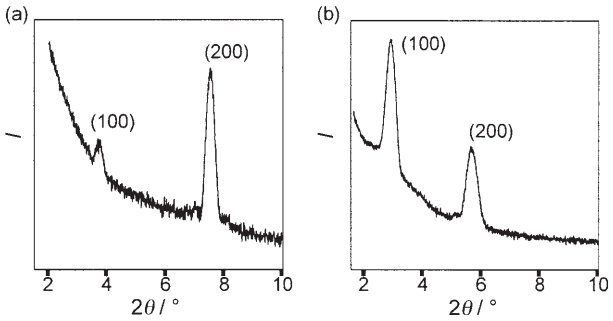

Figure 9. XRD patterns of vacuum-deposited thin films of a) **DE-SOSOS** and b) **DH-SOSOS** on Si/SiO_2 substrates.

31.5 Å on the basis of the X-ray structure, the molecule is considered to be arranged with a tilt angle of 14°, that is, nearly perpendicular to the substrate but tilted from the normal by 14° (assuming that the molecular length is the same in the crystal and in the film).[24] Therefore, the molecules **DE-SOSOS** and **DH-SOSOS** in the present work are supposed to be more perpendicular to the substrate than α,α′-dihexylquinquethiophene, whose tilt angle was reported to be around 30°.[2h,3c] For the films of alkylated longer-chain oligomers **DE-SOSOSOS** and **DH-SOSOSOS**, only amorphous morphology was observed, probably due to their greater molecular flexibility relative to the oligomers with shorter chain length (Figure 8 f).

The morphologies of the thin films obtained by spin coating exhibited a similar trend to those obtained by vacuum deposition (Table 4). Thin films of **SOSOS** and **DH-SOSOSOS** were amorphous, whereas those of **SOSOSOS** and **DH-SOSOS** had layer-by-layer arrangements (Figure 10 a–c). As with the case of vacuum-deposited films, the XRD pattern of the spin-coated film of **SOSOSOS** did not show a clear peak, but that of the thin film of **DH-SOSOS** showed a diffraction peak at $2\theta = 2.54°$ (100) (Figure 10 d), corresponding to a *d* spacing of 34.7 Å, which is longer than the molecular length (31.5 Å) in the crystal structure. This may be due to the possible stretching of the hexyl group in the film relative to that in the densely packed crystal form. It may be concluded that the film morphologies depend highly on the length of the molecule.

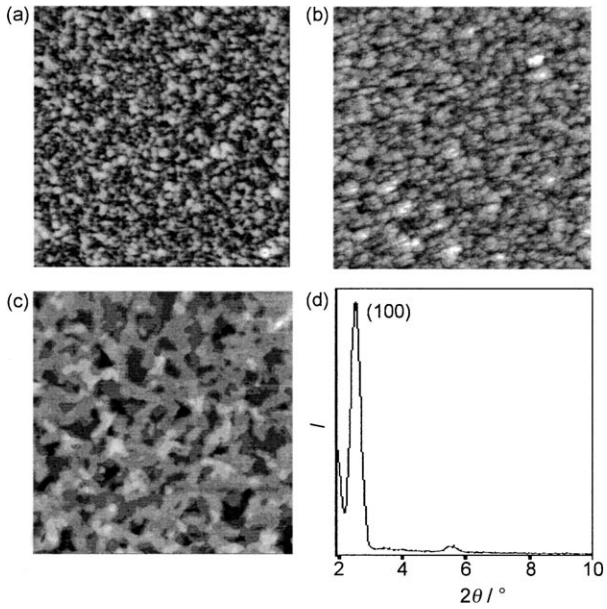

Figure 10. AFM images of thin films formed by spin coating. a) **DH-SOSOSOS** ($10 \times 10\ \mu m^2$), b) **SOSOSOS** ($10 \times 10\ \mu m^2$), and c) **DH-SOSOS** ($2 \times 2\ \mu m^2$). d) XRD pattern of spin-coated thin films of **DH-SOSOS** on Si/SiO_2 substrate.

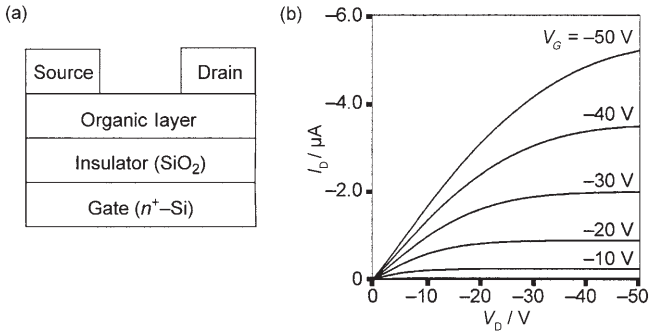

Figure 11. a) Schematic cross-section of a top-contact-type FET device. b) Drain-source current (I_D) versus drain-source voltage (V_D) observed for **DH-SOSOS** with octadecyltrichlorosilane (OTS)-modified SiO_2 substrate.

OFET Characteristics

Finally, OFET devices with the top-contact structure were constructed by using a series of oligo(thienylfuran)s on Si/SiO_2 substrates (Figure 11 a). The FET measurements for the devices prepared by vacuum deposition and spin coating were carried out under vacuum (10^{-3} Pa) and in air, respectively, at room temperature (see Experimental Section for details). All the OFET devices prepared in this way showed the p-type transistor response. As an example, the source-drain current (I_D) versus source-drain voltage (V_D) curves for the different gate voltages (V_G), obtained by an OFET device made of **SOSOSO** film deposited under vacuum, are shown in Figure 11 b. The field-effect mobility (μ) was determined by using the saturation region. The observed FET performance of each oligomer measured on the films prepared as mentioned above is summarized in Table 5.

As shown in Table 5, the carrier mobilities of the vacuum-deposited films with the parent oligomers increase with an increase in the chain length of the oligomer, in agreement with the case of the parent α-oligothiophenes.[2h] However, not much change in carrier mobility was observed between the oligomers with odd and even numbers of heterocycles. The mobility of **SOSOSOS** was enhanced by nearly five times that of **SOSOS** and two times that of **SOSOSO**, probably owing to its better film morphology. The FET devices based on the α,α′-alkylated oligomers showed higher mobilities than those made of the corresponding parent oligomers.

Table 5. Field-effect mobility (μ), on/off ratio, and threshold voltage (V_T) for transistors of the oligomers prepared by vacuum deposition and spin coating.

Compound	Vacuum deposition[a]			Spin coating[b]		
	μ [$cm^2V^{-1}s^{-1}$]	on/off ratio	V_T [V]	μ [$cm^2V^{-1}s^{-1}$]	on/off ratio	V_T [V]
SOSOS[c]	2.6×10^{-4}	10^4	−54	–[d]	–[e]	–[e]
SOSOSO[c]	5.6×10^{-4}	10^5	−20	–[e]	–[e]	–[e]
SOSOSOS[c]	1.3×10^{-3}	10^4	−23	2.0×10^{-4}	10^2	−15
DE-SOSOS[c]	1.3×10^{-2}	10^4	−21	–[e]	–[e]	–[e]
DH-SOSOS[c]	1.4×10^{-2}	10^4	−26	1.0×10^{-3}	10^3	+8
DH-SOSOS[f]	3.6×10^{-2}	10^3	−2	–[e]	–[e]	–[e]
DE-SOSOSOS[c]	5.9×10^{-3}	10	−3	–[e]	–[e]	–[e]
DH-SOSOSOS[c]	5.7×10^{-3}	10	−21	5.7×10^{-6}	10	+31

[a] Measured under vacuum (10^{-3} Pa). The substrate temperatures were 40–60 °C.[26] [b] Measured in air. [c] With bare SiO_2 substrate. [d] No field-effect behavior observed. [e] Not determined. [f] With OTS-modified SiO_2 substrate.

Notably, the mobilities of **DE-SOSOS** and **DH-SOSOS** were enhanced by almost two orders of magnitude relative to that of unsubstituted **SOSOS**. On the other hand, the enhancement of the mobilities of **DE-SOSOSOS** and **DH-SOSOSOS** was not as great relative to **SOSOSOS**, thus reflecting the poor film morphologies of **DE-SOSOSOS** and **DH-SOSOSOS**. Therefore, the FET devices based on **DE-SOSOS** and **DH-SOSOS** exhibited the highest mobilities, that is, $\mu=(1.3\text{–}1.4)\times10^{-2}\,cm^2V^{-1}s^{-1}$, among the series of oligomers in the present study, although their on/off ratios were low. However, when a device was fabricated with a vacuum-deposited thin film by using **DH-SOSOS** on a SiO_2 substrate treated with OTS, the field-effect mobility and the on/off ratio was 2.6 times and two orders of magnitude, respectively, higher than the values obtained by a device with the same film deposited on an unmodified SiO_2 substrate.

As a whole, the field-effect mobilities are known to be one to three orders of magnitude lower for devices fabricated with films made by spin coating than those made by vacuum deposition, generally due to poor film morphology. The film of **SOSOS** showed no field-effect behavior for the device when the film was made by spin coating; however, the devices made with vacuum-deposited film exhibited a mobility of $2.6\times10^{-4}\,cm^2V^{-1}s^{-1}$. When the film was made by spin coating, the field-effect mobility of the device with **SOSOSOS** ($2.0\times10^{-4}\,cm^2V^{-1}s^{-1}$) was higher than that with the dihexyl derivative **DH-SOSOSOS** ($5.7\times10^{-6}\,cm^2V^{-1}s^{-1}$), which is contrary to the trend for the vacuum-deposited film (**SOSOSOS** 1.3×10^{-3}, **DH-SOSOSOS** $5.7\times10^{-3}\,cm^2V^{-1}s^{-1}$). Thus, a change in film morphology, which is dependent on molecular length, affects the performance of FET devices more evidently for films made by spin coating rather than vacuum deposition. On the other hand, the device made from **DH-SOSOS** showed the highest level of mobility among those fabricated by spin coating (μ(**DH-SOSOS**) $1.0\times10^{-3}\,cm^2V^{-1}s^{-1}$)[25] as well as those made with vacuum-deposited films (μ(**DH-SOSOS**) $1.4\times10^{-2}\,cm^2V^{-1}s^{-1}$); this result is apparently due to the superb morphology developed in that film.

Conclusions

A newly synthesized series of alternately connected thiophene–furan oligomers with thiophene rings at both ends, **SOSOSOS**, **DE-SOSOS**, **DH-SOSOS**, **DE-SOSOSOS**, and **DH-SOSOSOS**, were found to have advantages such as higher solubility over oligothiophenes. In the UV/Vis absorption spectra, the maximum absorptions of these oligo(thienylfuran)s exhibited bathochromic shifts with increasing chain length, and the absorption as well as the calculated HOMO–LUMO gap was nearly constant regardless of chain length and the composition of the heterocyclic components. The results of the electrochemical measurements are also in agreement with the prediction that the oxidation potential generally becomes lower with increasing chain length, with an accompanying increase in the HOMO level. The crystal structures of **DE-SOSOS** and **DH-SOSOS** revealed that the π systems have slightly bent but almost planar structures with more densely packed herringbone arrangements than those of pentacene, α-sexithiophene, and α,α′-dimethylquaterthiophene. The morphologies of the thin films of the oligomers prepared by vacuum deposition and by a solution process showed great dependence on the molecular length, and the films of **DE-SOSOS** and **DH-SOSOS** showed highly ordered arrangements with a nearly vertical orientation with respect to the substrate. These arrangements are reflected in relatively good FET mobilities, which indicate that the oligomers containing furan rings can be applied to the active layer of OFET devices fabricated by both vacuum deposition and by the solution process. The FET performance of the device with the film of **DH-SOSOS** deposited on an OTS-treated SiO_2 substrate was considerably improved. The results of the present study would be useful in the future molecular design of more-effective OFET devices composed of various conjugated heterocyclic rings.

Experimental Section

General

Melting points were determined on a Yanaco MP-500D apparatus and are uncorrected. Elemental analysis was performed at the Microanalysis Division of Institute for Chemical Research, Kyoto University. ^1H (300 MHz) and ^{13}C NMR (75.4 MHz) spectra were recorded on a Varian Mercury-300 spectrometer. Chemical shifts are reported in ppm with reference to tetramethylsilane and with the solvent signals as internal standard ($\delta=7.26$ ppm for $CHCl_3$ in ^1H NMR, $\delta=77.2$ ppm for $CDCl_3$ in ^{13}C NMR). Preparative gel-permeation chromatography (GPC) was performed with JAI LC-908 and LC-918 chromatographs equipped with JAIGEL 1H and 2H columns. UV/Vis spectra were recorded on a Shimadzu UV-3150 spectrometer. Mass spectra were obtained on a JEOL JMS700 spectrometer. AFM images of thin films vacuum-deposited and spin-coated onto Si/SiO_2 substrates were obtained by using a Digital Instruments Nanoscope IIIa microscope and a SII Nano Technology SPI3800N-SPA400 microscope, respectively, in air. Ultraviolet ozone cleaner is a commercial product of Nippon Laser & Electronics Lab (NL-UV253S).

All reactions were carried out under argon atmosphere unless otherwise noted. One drop of Et_3N was added to all solvents used for the workup procedures. For cross-coupling reactions, THF and DMF supplied from

Wako Co. as dry solvents were employed. All commercially available materials were of reagent grade unless otherwise noted. Compound **4c**[13] and oligomer **SOSOS**[12b] were synthesized according to procedures in the literature. The SiO_2 substrate was thermally grown by Miyazaki Oki Electric Co., Ltd. by using a highly doped n^+-Si wafer purchased from International Test & Engineering Services Co., Ltd.

Computational Methods

All calculations were performed with the Gaussian 98 programs.[27] Geometry optimizations were performed with the restricted Becke hybrid (B3LYP) at the 6–31G(d) level. The HOMO and LUMO levels were estimated with single-point calculations (B3LYP/6–311+G(2d,p)) by using the geometries optimized at the B3LYP/6–31G(d) level.

Syntheses

2a: NBS (16.3 g, 91.6 mmol) was added in one portion to a stirred solution of 2-ethylthiophene (**1a**; 10.3 g, 91.6 mmol) in AcOH (40 mL). The mixture was stirred for 1 h at room temperature. The reaction was quenched with water (20 mL), and the mixture was extracted with diethyl ether, washed with aqueous NaOH (1 M), and the organic layer was dried over $MgSO_4$. The solvent was removed in vacuo to afford 2-bromo-5-ethylthiophene (**2a**; 13.87 g, 79.3 %) as a colorless oil. ^{1}H NMR ($CDCl_3$): δ = 6.84 (d, J = 3.8 Hz, 2H), 6.54 (d, J = 3.8 Hz, 2H), 2.78 (q, J = 7.5 Hz, 2H), 1.29 ppm (t, J = 7.5 Hz, 3H); ^{13}C NMR ($CDCl_3$): δ = 149.2, 129.5, 123.8, 108.7, 23.8, 15.9 ppm; HRMS (EI): m/z calcd for C_6H_7BrS: 189.9452; found: 189.9445.

2b: 2-Bromo-5-hexylthiophene (**2b**) was prepared in the same way as **2a**. The use of 2-hexylthiophene (**1b**; 9.64 g, 57.3 mmol), NBS (10.3 g, 57.6 mmol), and AcOH (20 mL) gave **2b** (13.9 g, 97.9 %) as a colorless oil. The ^{1}H and ^{13}C NMR spectral data were identical to those reported.[28]

3a: A mixture of **2a** (13.7 g, 71.7 mmol), [Pd(PPh_3)$_4$] (4.10 g, 3.54 mmol), and CuO (5.70 g, 71.7 mmol) in dry DMF (100 mL) was stirred at 100 °C. After 5 min, 2-(tributylstannyl)furan (24.7 mL, 75.3 mmol) was added. The mixture was stirred at 100 °C for 1 h and then cooled to room temperature. The precipitates were filtered off, and the volatiles of the filtrate were removed in vacuo. The residue was purified by flash chromatography over SiO_2 with hexane as an eluent to afford 2-ethyl-5-(2′-furyl)thiophene (**3a**; 9.70 g, 75.9 %) as a pale-yellow oil. ^{1}H NMR ($CDCl_3$): δ = 7.34 (m, 1H), 7.04 (d, J = 3.5 Hz, 1H), 6.68 (d, J = 3.5 Hz, 1H), 6.38 (m, 2H), 2.82 (q, J = 7.6 Hz, 2H), 1.30 ppm (t, J = 7.6 Hz, 3H); ^{13}C NMR ($CDCl_3$): δ = 150.0, 146.9, 141.4, 131.3, 124.1, 122.5, 111.7, 104.4, 23.62, 16.10 ppm; HRMS (EI): m/z calcd for $C_{10}H_{10}OS$: 178.0452; found: 178.0451.

3b: 2-(2′-Furyl)-5-hexylthiophene (**3b**) was prepared in the same way as **3a**. The use of **2b** (1.00 g, 4.05 mmol), [Pd(PPh_3)$_4$] (0.100 g, 0.087 mmol), CuO (0.322 g, 4.05 mmol), DMF (11 mL), and 2-(tributylstannyl)furan (2.0 mL, 6.08 mmol) gave **3b** (948 mg, quant.) as a pale-yellow oil. ^{1}H NMR ($CDCl_3$): δ = 7.37 (m, 1H), 7.05 (d, J = 3.6 Hz, 1H), 6.69 (d, J = 3.6 Hz, 1H), 6.42–6.39 (m, 2H), 2.79 (t, J = 7.5 Hz, 2H), 1.68 (m, 2H), 1.42–1.26 (m, 6H), 0.89 ppm (t, J = 6.9 Hz, 3H); ^{13}C NMR ($CDCl_3$): δ = 150.0, 145.4, 141.4, 131.3, 124.8, 122.5, 111.7, 104.4, 31.81, 31.79, 30.28, 28.95, 22.80, 14.30 ppm; HRMS (EI): m/z calcd for $C_{14}H_{18}OS$: 234.1078; found: 234.1094; elemental analysis: calcd (%) for $C_{14}H_{18}OS$: C 71.75, H 7.74; found: C 71.57, H 7.87.

5a: NBS (4.80 g, 27.0 mmol) was gradually added to a stirred solution of **3a** (4.82 g, 27.0 mmol) and BPO (10 mg) in toluene (300 mL) over 30 min at −10 °C in air in the dark. After the mixture was stirred for 0.5 h at −10 °C, the solvent was evaporated in vacuo. The residue was subjected to flash chromatography over SiO_2 with hexane as an eluent to afford 2-{2′-(5′-bromofuryl)}-5-ethylthiophene (**4a**) as a colorless oil. ^{1}H NMR ($CDCl_3$): δ = 7.04 (d, J = 3.8 Hz, 1H), 6.70 (d, J = 3.8 Hz, 1H), 6.35 (d, J = 3.2 Hz, 1H), 6.32 (d, J = 3.2 Hz, 1H), 2.84 (q, J = 10.3 Hz, 2H), 1.31 ppm (t, J = 10.3 Hz, 3H). Because of its instability, **4a** was used in the next step without further purification. 2-{2′-(5′-Ethylthienyl)}-5-(2′-thienyl)furan (**5a**) was prepared in the same way as **3a**. The use of **4a**, 2-(tributylstannyl)thiophene (8.6 mL, 27.1 mmol), [Pd(PPh_3)$_4$] (1.60 g, 1.38 mmol), CuO (2.20 g, 27.7 mmol), and DMF (100 mL) gave **5a** (4.64 g, 66.0 %) as a pale-yellow oil. ^{1}H NMR ($CDCl_3$): δ = 7.27 (dd, J = 3.7, 1.0 Hz, 1H), 7.20 (dd, J = 5.2, 1.0 Hz, 1H), 7.10 (d, J = 3.6 Hz, 1H), 7.02 (dd, J = 5.2, 3.7 Hz, 1H), 6.71 (d, J = 3.6 Hz, 1H), 6.50 (d, J = 3.6 Hz, 1H), 6.43 (d, J = 3.6 Hz, 1H), 2.84 (q, J = 7.5 Hz, 2H), 1.32 ppm (t, J = 7.5 Hz, 3H); ^{13}C NMR ($CDCl_3$): δ = 149.0, 148.4, 147.1, 133.8, 130.9, 127.8, 124.2, 124.1, 122.7, 122.6, 107.3, 106.5, 23.7, 16.1 ppm; HRMS (EI): m/z calcd for $C_{14}H_{12}OS_2$: 260.0330; found: 260.0331.

5b: 2-{2′-(5′-Bromofuryl)}-5-hexylthiophene (**4b**) was prepared in the same way as **4a**. The use of **3b** (0.524 g, 2.23 mmol), NBS (0.639 g, 3.59 mmol), BPO (5 mg), and toluene (50 mL) gave **4b** as a colorless oil. ^{1}H NMR ($CDCl_3$): δ = 7.04 (d, J = 3.6 Hz, 1H), 6.68 (d, J = 3.3 Hz, 1H), 6.35 (d, J = 3.6 Hz, 1H), 6.32 (d, J = 3.3 Hz, 1H), 2.80 (t, J = 7,5 Hz, 2H), 1.74–1.62 (m, 2H), 1.37–1.26 (m, 6H), 0.89 ppm (t, J = 7.2 Hz, 3H). Because of its instability, **4b** was used in the next step without further purification. A mixture of **4b**, 2-(tributylstannyl)thiophene (0.71 mL, 2.24 mmol), and [Pd(PPh_3)$_4$] (98.8 mg, 0.09 mmol) in THF (30 mL) was stirred at 60 °C for 2 days. The reaction was quenched with water (20 mL), the mixture was extracted with diethyl ether, and the organic layer was dried over $MgSO_4$. The solvent was removed in vacuo, and the residue was purified by column chromatography over SiO_2 eluted with hexane to afford 2-{2′-(5′-hexylthienyl)}-5-(2′-thienyl)furan (**5b**; 537 mg, 76.0 %) as a yellow oil. ^{1}H NMR ($CDCl_3$): δ = 7.29 (dd, J = 3.6, 1.2 Hz, 1H), 7.22 (dd, J = 5.1, 1.2 Hz, 1H), 7.12 (d, J = 3.5 Hz, 1H), 7.05 (dd, J = 5.1, 3.6 Hz, 1H), 6.72 (d, J = 3.5 Hz, 1H), 6.53 (d, J = 3.6 Hz, 1H), 6.46 (d, 3.6 Hz, 1H), 2.82 (t, J = 7.5 Hz, 2H), 1.74–1.65 (m, 2H), 1.44–1.27 (m, 6H), 0.90 ppm (t, J = 6.9 Hz, 3H); ^{13}C NMR ($CDCl_3$): δ = 149.0, 148.3, 145.6, 133.8, 131.0, 127.9, 124.2, 122.7, 122.6, 107.3, 106.5, 31.8, 31.8, 30.3, 29.0, 22.8, 14.3 ppm; HRMS (EI): m/z calcd for $C_{18}H_{20}OS_2$: 316.0956; found: 316.0967; elemental analysis: calcd (%) for $C_{18}H_{20}OS_2$: C 68.31, H 6.37; found: C 68.41, H 6.50.

5c: A mixture of 2-{2′-(5′-bromofuryl)}-5-(trimethylsilyl)thiophene (**4c**; 1.57 g, 5.21 mmol), 2-(tributylstannyl)thiophene (2.4 mL, 7.57 mmol), and [Pd(PPh_3)$_4$] (115 mg, 0.10 mmol) in THF (60 mL) was stirred at 60 °C for 2 days. The reaction was quenched with water (60 mL), the mixture was extracted with diethyl ether, and the organic layer was dried over $MgSO_4$. The solvent was removed in vacuo, and the residue was purified by column chromatography over SiO_2 eluted with hexane/CH_2Cl_2 (20:1) to afford 2-[2′-{5′-(trimethysilyl)thienyl}]-5-(2′-thienyl)furan (**5c**; 1.01 g, 63.4 %) as a yellow oil. ^{1}H NMR ($CDCl_3$): δ = 7.35 (d, J = 3.6 Hz, 1H), 7.31 (dd, J = 3.6 , 1.1 Hz, 1H), 7.23 (dd, J = 5.1, 1.1 Hz, 1H) , 7.16 (d, J = 3.6 Hz, 1H), 7.05 (dd, J = 5.1, 3.6 Hz, 1H), 6.56–6.52 (m, 2H), 0.34 ppm (s, 9H); ^{13}C NMR ($CDCl_3$): δ = 148.9, 148.8, 139.7, 138.5, 134.8, 133.7, 127.9, 124.4, 124.1, 122.9, 107.5, 107.4, 0.1 ppm; HRMS (EI): m/z calcd for $C_{15}H_{16}OS_2Si$: 304.0412; found: 304.0408; elemental analysis: calcd (%) for $C_{15}H_{16}OS_2Si$: C 59.17, H 5.30; found: C 59.37, H 5.32.

DE-SOSOS: A solution of LDA in cyclohexane (1.5 M, 4.1 mL, 6.15 mmol) was added dropwise to a stirred solution of **5a** (1.56 g, 5.99 mmol) in THF (50 mL) at −78 °C. The mixture was warmed to 0 °C over a period of 5 min and recooled to −78 °C. Tributyltin chloride (1.9 mL, 6.65 mmol) was added at −78 °C, and the reaction mixture was stirred for 2 h at room temperature. The solvent was removed in vacuo, and DMF (10 mL) was added to the residue. This solution was added to a mixture of [Pd(PPh_3)$_4$] (444 mg, 0.38 mmol), CuO (610 mg, 7.67 mmol), and **4a**, which was prepared by treatment of **3a** (1.37 g, 7.67 mmol) with NBS (1.43 g, 8.05 mmol) and BPO (10 mg) in toluene (100 mL) as described above, in DMF (40 mL), which was stirred for 5 min at 100 °C. The entire reaction mixture was stirred for 1 h at 100 °C and then cooled to room temperature. The precipitates were filtered off, and the volatiles of the filtrate were removed in vacuo. Water (20 mL) and diethyl ether (30 mL) were added to the residue, and the aqueous layer was extracted with diethyl ether. The organic layer was dried over $MgSO_4$. The solvent was removed in vacuo, and the crude product was purified by preparative GPC eluted with toluene to afford **DE-SOSOS** (1.66 g, 64.4 %) as a yellow solid. An analytically pure sample was obtained by reprecipitation from hexane and CH_2Cl_2. M.p.: 109.5–110.5 °C; ^{1}H NMR ($CDCl_3$): δ = 7.19 (s, 2H), 7.12 (d, J = 3.6 Hz, 2H), 6.72 (d, J = 3.6 Hz, 2H), 6.52 (d, J = 3.5 Hz, 2H), 6.45 (d, J = 3.5 Hz, 2H), 2.85 (q, J = 7.5 Hz, 4H), 1.33 ppm (t, J = 7.5 Hz, 6H); ^{13}C NMR ($CDCl_3$): δ = 149.2, 148.5, 147.2, 132.0,

130.8, 124.3, 123.1, 122.8, 107.6, 106.7, 23.7, 16.1 ppm; HRMS (EI): *m/z* calcd for $C_{24}H_{20}O_2S_3$: 436.0625; found: 436.0638; elemental analysis: calcd (%) for $C_{24}H_{20}O_2S_3$: C 66.02, H 4.62; found: C 66.05, H 4.51.

DH-SOSOS: A solution of LDA was prepared as follows. A solution of *n*-butyllithium in hexane (1.54 M, 2.25 mL, 3.47 mmol) was added dropwise to a stirred solution of diisopropylamine (1.79 mL, 12.8 mmol) in THF (4.2 mL) at −78 °C. The stirred mixture was warmed to 0 °C over 10 min and recooled to −78 °C. A suspension of **5b** (893 mg, 2.83 mmol) and tributyltin chloride (1.25 mL, 4.61 mmol) in THF (5 mL) was added dropwise to this solution by cannula, and the mixture was stirred at room temperature for 2 h. A solution of **4b**, which was prepared by treatment of **3b** (460 mg, 1.96 mmol) with NBS (356 mg, 2.00 mmol) and a small portion of BPO in toluene (30 mL) as described above, in THF (20 mL) was added to this mixture by cannula, followed by $[Pd(PPh_3)_4]$ (58 mg, 0.05 mmol). The reaction mixture was stirred for 3 days at 70 °C. The reaction was quenched with water (20 mL), the mixture was extracted with diethyl ether, and the organic layer was dried over $MgSO_4$. The solvent was removed in vacuo, and recrystallization of the residue from hexane and CH_2Cl_2 gave **DH-SOSOS** (658 mg, 42.4 %) as a yellow solid. M.p.: 95.5–96.5 °C; ^{1}H NMR ($CDCl_3$): δ = 7.20 (s, 2H), 7.12 (d, J = 3.6 Hz, 2H), 6.72 (d, J = 3.6 Hz, 2H), 6.54 (d, J = 3.5 Hz, 2H), 6.46 (d, J = 3.5 Hz, 2H), 2.81 (t, J = 7.7 Hz, 4H), 1.74–1.64 (m, 4H), 1.41–1.28 (m, 12H), 0.90 ppm (t, J = 6.9 Hz, 6H); ^{13}C NMR ($CDCl_3$): δ = 149.2, 148.1, 145.7, 132.0, 130.9, 125.0, 123.2, 122.7, 107.6, 106.7, 31.8, 31.8, 30.4, 29.0, 22.8, 14.3 ppm; HRMS (EI): *m/z* calcd for $C_{32}H_{36}O_2S_3$: 548.1877; found: 548.1877; elemental analysis: calcd (%) for $C_{32}H_{36}O_2S_3$: C 70.03, H 6.61; found: C 70.20, H 6.72.

DE-SOSOSOS: A solution of LDA in cyclohexane (1.5 M, 4.0 mL, 6.00 mmol) was added dropwise to a stirred solution of **5a** (1.56 g, 5.99 mmol) in THF (50 mL) at −78 °C. The mixture was warmed to 0 °C over 5 min and recooled to −78 °C. Tributyltin chloride (1.8 mL, 6.30 mmol) was added at −78 °C, and the reaction mixture was stirred for 2 h at room temperature. The solvent was removed in vacuo, and DMF (10 mL) was added to the residue. This solution was added to a mixture of 2,5-dibromofuran (726 mg, 3.0 mmol), $[Pd(PPh_3)_4]$ (347 mg, 0.30 mmol), and CuO (477 mg, 6.00 mmol) in DMF (40 mL), which was stirred for 5 min at 100 °C. The entire reaction mixture was stirred for 1 h at 100 °C and then cooled to room temperature. The precipitates were filtered off, and the volatiles of the filtrate were removed in vacuo. Water (20 mL) and diethyl ether (30 mL) were added to the residue, and the two layers were separated. After extraction of the aqueous layer with diethyl ether, the organic layer was dried over $MgSO_4$. The solvent was removed in vacuo, and the crude product was further purified by preparative GPC eluted with toluene to afford **DE-SOSOSOS** (1.19 g, 67.9 %) as a brown solid. An analytically pure sample was obtained by reprecipitation from hexane and CH_2Cl_2. M.p.: 172.9–174.3 °C; ^{1}H NMR ($CDCl_3$): δ = 7.23 (d, J = 3.9 Hz, 2H), 7.21 (d, J = 3.9 Hz, 2H), 7.13 (d, J = 3.6 Hz, 2H), 6.74 (d, J = 3.6 Hz, 2H), 6.57 (s, 2H), 6.55 (d, J = 3.5 Hz, 2H), 6.47 (d, J = 3.5 Hz, 2H), 2.86 (q, J = 7.5 Hz, 4H), 1.34 ppm (t, J = 7.5 Hz, 6H); ^{13}C NMR ($CDCl_3$): δ = 149.3, 148.6, 148.0, 147.3, 132.4, 131.7, 130.8, 124.3, 123.5, 123.2, 122.8, 107.8, 107.7, 106.8, 23.7, 16.1 ppm; HRMS (EI): *m/z* calcd for $C_{32}H_{24}O_3S_4$: 584.0608; found: 584.0641.

DH-SOSOSOS: A solution of LDA was prepared as follows. A solution of *n*-butyllithium in hexane (1.47 M, 2.5 mL, 3.68 mmol) was added dropwise to a stirred solution of diisopropylamine (0.58 mL, 4.14 mmol) in THF (2.8 mL) at −78 °C. The mixture was warmed to 0 °C over 10 min and recooled to −78 °C. A mixture of **5b** (628 mg, 1.99 mmol) and tributyltin chloride (0.98 mL, 3.61 mmol) in THF (7.5 mL) was added dropwise by cannula, and the mixture was warmed to room temperature for 2 h. 2,5-Dibromofuran (202 mg, 0.89 mmol) and $[Pd(PPh_3)_4]$ (80 mg, 0.07 mmol) were added to this mixture. The reaction mixture was stirred for 3 days at 70 °C. The reaction was quenched with water (20 mL), the mixture was extracted with diethyl ether, and the organic layer was dried over $MgSO_4$. The solvent was removed in vacuo, and recrystallization of the residue from hexane and CH_2Cl_2 gave **DH-SOSOSOS** (273 mg, 39.3 %) as a yellow solid. M.p.: 137.3–139.1 °C ; ^{1}H NMR ($CDCl_3$): δ = 7.22 (d, J = 3.8 Hz, 2H), 7.19 (d, J = 3.8 Hz, 2H), 7.12 (d, J = 3.6 Hz, 2H), 6.71 (d, J = 3.6 Hz, 2H), 6.55 (s, 2H), 6.54 (d, J = 3.5 Hz, 2H), 6.46 (d, J = 3.5 Hz, 2H), 2.81 (t, J = 7.5 Hz, 4H), 1.74–1.64 (m, 4H), 1.40–1.29 (m, 12H), 0.92 ppm (t, J = 6.8 Hz, 6H); ^{13}C NMR ($CDCl_3$): δ = 149.3, 148.6, 148.0, 145.8, 132.4, 131.7, 130.9, 125.0, 123.5, 123.2, 122.8, 107.8, 107.8, 106.8, 31.8, 31.8, 30.4, 29.0, 22.8, 14.3 ppm; HRMS (EI): *m/z* calcd for $C_{40}H_{40}O_3S_4$: 696.1860; found: 696.1879; elemental analysis: calcd (%) for $C_{40}H_{40}O_3S_4$: C 68.93, H 5.78; found: C 68.71, H 5.76.

DTMS-SOSOSOS: A solution of *n*-butyllithium in hexane (1.55 M, 3.68 mL, 5.70 mmol) was added dropwise to a stirred solution of **5c** (1.49 g, 4.90 mmol) and *N,N,N′,N′*-tetramethylethylenediamine (0.82 mL) in THF (48 mL) at −78 °C. The mixture was stirred at −78 °C for 15 min and then at room temperature for 1 h. After the mixture was cooled to −78 °C again, a solution of tributyltin chloride (1.54 mL, 5.68 mmol) was added, and the reaction mixture was stirred at room temperature for 3 h. 2,5-Dibromofuran (539 mg, 2.38 mmol) and $[Pd(PPh_3)_4]$ (223 mg, 0.19 mmol) were added to this mixture. The reaction mixture was stirred for 3 days at 70 °C. The reaction was quenched with water (20 mL), the mixture was extracted with diethyl ether, and the organic layer was dried over $MgSO_4$. The solvent was removed in vacuo, and recrystallization of the residue from ethanol/CH_2Cl_2 (3:2) gave **DTMS-SOSOSOS** (433 mg, 26.2 %) as a brown solid. M.p.: 189.6–190.8 °C; ^{1}H NMR ($CDCl_3$): δ = 7.37 (d, J = 3.5 Hz, 2H), 7.24 (m, 4H), 7.17 (d, J = 3.5 Hz, 2H), 6.58–6.65 (m, 6H), 0.35 ppm (s, 18H); ^{13}C NMR ($CDCl_3$): δ = 149.1, 148.6, 148.4, 139.9, 138.3, 134.9, 132.2, 131.9, 124.2, 123.6, 123.4, 107.9, 107.8, 107.7, 0.1 ppm; HRMS (FAB): *m/z* calcd for $C_{34}H_{32}O_3S_4Si_2$: 672.0773; found: 672.0768.

SOSOSOS: A solution of TBAF (1.0 M, 3.6 mL, 3.6 mmol) in THF was added to a stirred solution of **DTMS-SOSOSOS** (1.21 g, 1.79 mmol) in wet THF (20 mL) in air. The reaction mixture was stirred for 0.5 h. The reaction was quenched with water (10 mL), the mixture was extracted with diethyl ether, and the organic layer was dried over $MgSO_4$. The solvent was removed in vacuo, and the crude product was further purified by preparative GPC eluted with $CHCl_3$ to afford **SOSOSOS** (0.503 g, 53.2 %) as an orange solid. M.p.: 179.4–181.3 °C; ^{1}H NMR ($CDCl_3$): δ = 7.33 (dd, J = 3.6, 0.9 Hz, 2H), 7.26–7.24 (m, 6H), 7.06 (dd, J = 4.8, 3.6 Hz, 2H), 6.59 (s, 2H), 6.58–6.56 ppm (m, 4H); ^{13}C NMR ($CDCl_3$): δ = 149.0, 148.6, 148.4, 133.5, 132.2, 132.0, 128.0, 124.6, 123.6, 123.5, 123.0, 107.9, 107.8, 107.6 ppm; HRMS (FAB): *m/z* calcd for $C_{28}H_{17}O_3S_4$: 527.9982; found: 527.9988; elemental analysis: calcd (%) for $C_{28}H_{16}O_3S_4$: C 63.61, H 3.05; found: C 63.43, H 2.99.

X-ray Diffraction[29]

X-ray diffraction of organic thin films vacuum-deposited and spin-coated onto the Si/SiO_2 substrate was conducted with a Rigaku RAD-IIB diffractometer with a $Cu_{K\alpha}$ source (λ = 1.541 Å) and a Rigaku RINT-TTRII diffractometer with a $Cu_{K\alpha}$ source (λ = 1.541 Å) in air, respectively. For X-ray crystallography, the intensity data were collected at 100 K on a Bruker SMART APEX diffractometer with $Mo_{K\alpha}$ radiation (λ = 0.71073 Å) and a graphite monochromater. The structure was solved by direct methods (SHELXTL) and refined by full-matrix least squares on F^2 (SHELXL-97). All non-hydrogen atoms were refined anisotropically, and all hydrogen atoms were placed by using AFIX instructions.

DH-SOSOS: Single crystals suitable for X-ray crystallography were obtained by sublimation at 200 °C under reduced pressure (≈133 Pa) for 10 days. $C_{32}H_{36}O_2S_3$, M_r = 548.79, crystal size 0.10 × 0.10 × 0.05 mm^3, monoclinic, $P2_1/n$, a = 7.416(3), b = 5.879(2), c = 64.92(2) Å, β = 91.815(6)°, V = 2828.9(17) Å^3, Z = 4, ρ_{calcd} = 1.289 g cm^{-3}. The refinement converged to R_1 = 0.1467, wR_2 = 0.2808 ($I > 2\sigma(I)$), GOF = 1.251.

DE-SOSOS: Single crystals suitable for X-ray crystallography were obtained by sublimation at 150 °C under reduced pressure (≈133 Pa) for 10 days. The terminal thiophene rings were disordered, and the occupancies of the E and E′ rings (Figure 5a and b) were refined as 0.75:0.25. $C_{24}H_{20}O_2S_3$, M_r = 436.58, crystal size 0.29 × 0.17 × 0.15 mm^3, orthorhombic, *Fdd*2, a = 32.160(8), b = 45.189(11), c = 5.7411(15) Å, V = 8344(4) Å^3, Z = 16, ρ_{calcd} = 1.390 g cm^{-3}. The refinement converged to R_1 = 0.0422, wR_2 = 0.0767 ($I > 2\sigma(I)$), GOF = 1.001.

Cyclic Voltammetry

CV was conducted with a BAS CV-50W electrochemical analyzer by using a standard three-electrode cell consisting of a glassy-carbon working electrode, a Pt-wire counter electrode, and an $Ag/AgNO_3$ (CH_3CN) reference electrode under argon atmosphere. Measurements were carried out with 1.0 mM solutions of samples in CH_2Cl_2 with tetrabutylammonium perchlorate as the supporting electrolyte (0.1 M) in all cases. The observed anodic peak potentials were calibrated with ferrocene added after each measurement.

FET Device Preparation

OFETs were fabricated in a top-contact manner as follows. For devices fabricated with a thin film made by vacuum deposition, the gate was a highly doped n^+-Si wafer, and the gate insulator was a 600-nm-thick layer of thermally grown SiO_2. After ultrasonication in acetone and then in isopropanol for 10 min each and treatment with ultraviolet ozone cleaner for 15 min to remove organic surface contaminants, the thin films of the oligomers (35 nm thick) were formed on SiO_2 by high-vacuum deposition (10^{-5} Pa) at substrate temperatures of 40–60 °C. Gold source and drain electrodes (40 nm thick) were thermally evaporated and deposited on the organic layer through a shadow mask. The channel length (L) and width (W) were 50 and 1000 μm, respectively. Devices prepared with films (30 nm thick) made from solutions of each oligomer in $CHCl_3$ or other solvents by spin-coating were fabricated with the gate insulator (200 nm thick), gold source, and drain electrodes (100 nm thick). The length and width of the channel was 50 μm and 5 mm, respectively. The I_D–V_D characteristics of the OFET devices were measured under vacuum (10^{-3} Pa) for the vacuum-deposited films by the use of a Keithley 6487 picoammeter for the drain and a Keithley 236 source measure unit for the gate, and in air for the spin-coated films by the use of an ADVANTEST CORPORATION R6245 power supply. Field-effect mobilities (μ) were calculated in the saturation region of I_D defined by the equation $I_D = (WC_i/2L)\mu(V_G - V_T)^2$, in which C_i is the capacitance of the SiO_2 insulator ($C_i = 5.8\times10^{-8}$ F cm^{-2} (600 nm thick) and 1.7×10^{-8} F cm^{-2} (200 nm thick)) and V_G and V_T are the gate and threshold voltages, respectively.

Acknowledgements

We thank Mr. Tatsuya Tanaka and Mr. Katsura Hirai (Konica Minolta Technology Center, Inc.) for preparation of spin-coated thin films and measurements of field-effect properties, AFM, and XRD of these films. We are also grateful to Dr. Daisuke Yamazaki (Institute for Chemical Research, Kyoto University) for his help in X-ray structural analysis. Y.M. thanks the JSPS for a Research Fellowship for Young Scientists.

[1] For examples, see: a) Y.-Y. Lin, D. J. Gundlach, S. F. Nelson, T. N. Jackson, *IEEE Electron Device Lett.* **1997**, *18*, 606; b) S. F. Nelson, Y.-Y. Lin, D. J. Gundlach, T. N. Jackson, *Appl. Phys. Lett.* **1998**, *72*, 1854; c) D. J. Gundlach, J. A. Nichols, L. Zhou, T. N. Jackson, *Appl. Phys. Lett.* **2002**, *80*, 2925; d) H. Klauk, M. Halik, U. Zschieschang, G. Schmid, W. Radlik, *J. Appl. Phys.* **2002**, *92*, 5259.

[2] For examples, see: a) F. Garnier, A. Yassar, R. Hajlaoui, G. Horowitz, F. Deloffre, B. Servet, S. Ries, P. Alnot, *J. Am. Chem. Soc.* **1993**, *115*, 8716; b) A. Dodabalapur, L. Torsi, H. E. Katz, *Science* **1995**, *268*, 270; c) R. Hajlaoui, D. Fichou, G. Horowitz, B. Nessakh, M. Constant, F. Garnier, *Adv. Mater.* **1997**, *9*, 557; d) F. Garnier, R. Hajlaoui, A. El Kassmi, G. Horowitz, L. Laigre, W. Porzio, M. Armanini, F. Provasoli, *Chem. Mater.* **1998**, *10*, 3334; e) G. Horowitz, M. E. Hajlaoui, *Adv. Mater.* **2000**, *12*, 1046; f) M. Halik, H. Klauk, U. Zschieschang, G. Schmid, S. Ponomarenko, S. Kirchmeyer, W. Weber, *Adv. Mater.* **2003**, *15*, 917; g) M. Manuela, M. Gazzano, G. Barbarella, M. Cavallini, F. Biscarini, P. Maccagnani, P. Ostoja, *J. Am. Chem. Soc.* **2003**, *125*, 10266; h) A. Facchetti, M. Mushrush, M.-H. Yoon, G. R. Hutchison, M. A. Ratner, T. J. Marks, *J. Am. Chem. Soc.* **2004**, *126*, 13859.

[3] a) H. E. Katz, A. J. Lovinger, J. G. Laquindanum, *Chem. Mater.* **1998**, *10*, 457; b) H. E. Katz, J. G. Laquindanum, A. J. Lovinger, *Chem. Mater.* **1998**, *10*, 633; c) W. Li, H. E. Katz, A. J. Lovinger, J. G. Laquindanum, *Chem. Mater.* **1999**, *11*, 458.

[4] a) H. E. Katz, A. Dodabalapur, L. Torsi, D. Elder, *Chem. Mater.* **1995**, *7*, 2238; b) H. E. Katz, W. Li, A. L. Lovinger, J. Laquindanum, *Synth. Met.* **1999**, *102*, 897; c) H. E. Katz, A. J. Lovinger, J. Johnson, C. Kloc, T. Siegrist, W. Li, Y.-Y. Lin, A. Dodabalapur, *Nature* **2000**, *404*, 478; d) S. A. Ponomarenko, S. Kirchmeyer, A. Elschner, B.-H. Huisman, A. Karbach, D. Drechsler, *Adv. Funct. Mater.* **2003**, *13*, 591; e) A. P. Kam, J. Seekamp, V. Solovyev, C. Clavijo Cedeno, A. Goldschmidt, C. M. Sotomayor Torres, *Microelectron. Eng.* **2004**, *73–74*, 809.

[5] T. Yamamoto, K. Takimiya, *J. Am. Chem. Soc.* **2007**, *129*, 2224.

[6] M. M. Payne, S. R. Parkin, J. E. Anthony, C.-C. Kuo, T. N. Jackson, *J. Am. Chem. Soc.* **2005**, *127*, 4986.

[7] B. A. Jones, M. J. Ahrens, M.-H. Yoon, A. Facchetti, T. J. Marks, M. R. Wasielewski, *Angew. Chem.* **2004**, *116*, 6523; *Angew. Chem. Int. Ed.* **2004**, *43*, 6363.

[8] a) T. M. Pappenfus, R. J. Chesterfield, C. D. Frisbie, K. R. Mann, J. Casado, J. D. Raff, L. L. Miller, *J. Am. Chem. Soc.* **2002**, *124*, 4184; b) R. J. Chesterfield, C. R. Newman, T. M. Pappenfus, P. C. Ewbank, M. H. Haukaas, K. R. Mann, L. L. Miller, C. D. Frisbie, *Adv. Mater.* **2003**, *15*, 1278.

[9] a) A. Facchetti, Y. Deng, A. Wang, Y. Koide, H. Sirringhaus, T. J. Marks, R. H. Friend, *Angew. Chem.* **2000**, *112*, 4721; *Angew. Chem. Int. Ed.* **2000**, *39*, 4547; b) A. Facchetti, M. Mushrush, H. E. Katz, T. J. Marks, *Adv. Mater.* **2003**, *15*, 33.

[10] A. Facchetti, M.-H. Yoon, C. L. Stern, H. E. Katz, T. J. Marks, *Angew. Chem.* **2003**, *115*, 4030; *Angew. Chem. Int. Ed.* **2003**, *42*, 3900.

[11] A. R. Murphy, J. M. J. Fréchet, P. Chang, J. Lee, V. Subramanian, *J. Am. Chem. Soc.* **2004**, *126*, 1596.

[12] a) L.-H. Chen, C.-Y. Wang, T.-M. H. Luo, *Heterocycles* **1994**, *38*, 1393; b) J. P. Parakka, M. P. Cava, *Synth. Met.* **1995**, *68*, 275; c) A. Hucke, M. P. Cava, *J. Org. Chem.* **1998**, *63*, 7413; d) F. Garzino, A. Méou, P. Brun, *Helv. Chim. Acta* **2002**, *85*, 1989; e) J. Seixas de Melo, F. Elisei, R. S. Becker, *J. Chem. Phys.* **2002**, *117*, 4428.

[13] Y. Miyata, T. Nishinaga, K. Komatsu, *J. Org. Chem.* **2005**, *70*, 1147.

[14] A. M. Eachern, C. Soucy, L. C. Leitch, J. T. Arnason, P. Morand, *Tetrahedron* **1988**, *44*, 2403.

[15] S. Gronowitz, P. Björk, J. Malm, A.-B. Hörnfeldt, *J. Organomet. Chem.* **1993**, *460*, 127.

[16] Determined in the present work.

[17] J. Nakayama, Y. Nakamura, T. Tajiri, M. Hoshino, *Heterocycles* **1986**, *24*, 637.

[18] a) P. Baüerle in *Electronic Materials: The Oligomeric Approach* (Eds.: K. Müllen, G. Wegner), Wiley-VCH, Weinheim, **1998**, chap. 2; b) A. Facchetti, M.-H. Yoon, C. L. Stern, G. R. Hutchison, M. A. Ratner, T. J. Marks, *J. Am. Chem. Soc.* **2004**, *126*, 13480.

[19] The CV behavior of **SOSOS** was reported earlier in reference [12c].

[20] a) S. Hotta, K. Waragai, *J. Mater. Chem.* **1991**, *1*, 835; b) G. Horowitz, B. Bachet, A. Yassar, P. Lang, F. Demanze, J.-L. Fave, F. Garnier, *Chem. Mater.* **1995**, *7*, 1337; c) C. Kloc, P. G. Simpkins, T. Siegrist, R. A. Laudise, *J. Cryst. Growth* **1997**, *182*, 416; d) T. Siegrist, C. Kloc, R. A. Laudise, H. E. Katz, R. C. Haddon, *Adv. Mater.* **1998**, *10*, 379; e) L. Antolini, G. Horowitz, F. Kouki, F. Garnier, *Adv. Mater.* **1998**, *10*, 382; f) J. Cornil, D. Beljonne, J.-P. Calbert, J. L. Brédas, *Adv. Mater.* **2001**, *13*, 1053; g) R. Azumi, M. Goto, K. Honda, M. Matsumoto, *Bull. Chem. Soc. Jpn.* **2003**, *76*, 1561.

[21] The standard vdW radii are taken from: A. Bondi, *J. Phys. Chem.* **1964**, *68*, 441.

[22] In our previous study,[13] DFT calculations (B3LYP/6–31G(d>)) indicated that both the *transoid* and *cisoid* forms of 2-(2′-thienyl)furan (**SO**) are completely planar (twist angle 0.0°), and that the *transoid* conformer is only 0.1 kcal mol^{-1} more stable than the *cisoid* conformer.

[23] The molecular length determined by X-ray crystallography was 22.4 Å.

[24] The tilt angle (θ_{tilt}) was calculated by $\theta_{tilt}=\cos^{-1}(d/l)$ ($d=d$ spacing from XRD, $l=$molecular length); see: K. Takimiya, Y. Kunugi, Y. Toyoshima, T. Otsubo, *J. Am. Chem. Soc.* **2005**, *127*, 3605.
[25] Annealing of the substrates of **DH-SOSOS** at 100 °C was carried out, but the field-effect property was not improved.
[26] For comparison, the FET measurement on α-sexithiophene afforded the values for mobility, on/off ratio, and V_T as 0.027 $cm^2V^{-1}s^{-1}$, 10^4, and −38 V, respectively.
[27] M. J. Frisch, G. W. Trucks, H. B. Schlegel, G. E. Scuseria, M. A. Robb, J. R. Cheeseman, V. G. Zakrzewski, J. A. Montgomery, Jr., R. E. Stratmann, J. C. Burant, S. Dapprich, J. M. Millam, A. D. Daniels, K. N. Kubin, M. C. Strain, O. Farkas, J. Tomasi, V. Barone, M. Cossi, R. Cammi, B. Mennucci, C. Pomelli, C. Adamo, S. Clifford, J. Ochterski, G. A. Petersson, P. Y. Ayala, Q. Cui, K. Morokuma, D. K. Malick, A. D. Rabuck, K. Raghavachari, J. B. Foresman, J. Cioslowski, J. V. Ortiz, B. B. Stefanov, G. Liu, A. Liashenko, P. Piskorz, I. Komaromi, R. Gomperts, R. L. Martin, D. J. Fox, T. Keith, M. A. Al-Laham, C. Y. Peng, A. Nanayakkara, C. Gonzalez, M. Challacombe, P. M. Gill, M. Head-Gordon, E. S. Replogle, J. A. Pople, Gaussian 98 (Revision A.5), Gaussian, Inc., Pittsburgh, PA (USA), **1998**.
[28] G. Barbarella, L. Favaretto, G. Sotgiu, M. Zambianchi, L. Antolini, O. Pudova, A. Bongini, *J. Org. Chem.* **1998**, *63*, 5497.
[29] CCDC-602719 (**DH-SOSOS**) and -602718 (**DE-SOSOS**) contain the supplementary crystallographic data for this paper. These data can be obtained free of charge from the Cambridge Crystallographic Data Centre, 12 Union Road, Cambridge CB2 1EZ, UK (fax: (+44) 1223-336-033; email: deposit@ccdc.cam.ac.uk) or at www.ccdc.cam.ac.uk/conts/retrieving.html.

Received: August 17, 2007
Published online: October 31, 2007

